Physiol Genomics 33: 361–372, 2008.
First published April 1, 2008; doi:10.1152/physiolgenomics.00139.2007.

Liver gene expression analysis reveals endoplasmic reticulum stress and metabolic dysfunction in SCD1-deficient mice fed a very low-fat diet

Matthew T. Flowers,[1,2] Mark P. Keller,[1] YounJeong Choi,[3] Hong Lan,[1] Christina Kendziorski,[3] James M. Ntambi,[1,2] and Alan D. Attie[1]

Departments of [1]Biochemistry, [2]Nutritional Sciences, and [3]Biostatistics and Medical Informatics, University of Wisconsin-Madison, Madison, Wisconsin

Submitted 3 July 2007; accepted in final form 27 March 2008

Flowers MT, Keller MP, Choi Y, Lan H, Kendziorski C, Ntambi JM, Attie AD. Liver gene expression analysis reveals endoplasmic reticulum stress and metabolic dysfunction in SCD1-deficient mice fed a very low-fat diet. *Physiol Genomics* 33: 361–372, 2008. First published April 1, 2008; doi:10.1152/physiolgenomics.00139.2007.—We previously reported that mice deficient in stearoyl-CoA desaturase-1 (*Scd1*) and maintained on a very low-fat (VLF) diet for 10 days developed severe loss of body weight, hypoglycemia, hypercholesterolemia, and many cholestasis-like phenotypes. To better understand the metabolic changes associated with these phenotypes, we performed microarray analysis of hepatic gene expression in chow- and VLF-fed female $Scd1^{+/+}$ and $Scd1^{-/-}$ mice. We identified an extraordinary number of differentially expressed genes (>4,000 probe sets) in the VLF $Scd1^{-/-}$ relative to both VLF $Scd1^{+/+}$ and chow $Scd1^{-/-}$ mice. Transcript levels were reduced for genes involved in detoxification and several facets of fatty acid metabolism including biosynthesis, elongation, desaturation, oxidation, transport, and ketogenesis. This pattern is attributable to the decreased mRNA abundance of several genes encoding key transcription factors, including LXRα, RXRα, FXR, PPARα, PGC-1β, SREBP1c, ChREBP, CAR, DBP, TEF, and HLF. A robust induction of endoplasmic reticulum (ER) stress is indicated by enhanced splicing of XBP1, increased expression of the stress-induced transcription factors CHOP and ATF3, and elevated expression of several genes involved in the integrated stress and unfolded protein response pathways. The gene expression profile is also consistent with induction of an acute inflammatory response and macrophage recruitment. These results highlight the importance of monounsaturated fatty acid synthesis for maintaining metabolic homeostasis in the absence of sufficient dietary unsaturated fat and point to a novel cellular nutrient-sensing mechanism linking fatty acid availability and/or composition to the ER stress response.

monounsaturated fatty acids; lipogenesis; cholestasis; microarray

STEAROYL-COA DESATURASE 1 (SCD1) is a central enzyme in lipid metabolism that catalyzes the Δ9-desaturation of the saturated fatty acids palmitate and stearate to the monounsaturated fatty acids (MUFA) palmitoleate and oleate, respectively (53). In the absence of SCD1 activity, as occurs in $Scd1^{-/-}$ mice, endogenous MUFA production is decreased, resulting in reduced lipid accumulation due to decreased fatty acid synthesis and increased fatty acid oxidation. The metabolic alterations in $Scd1^{-/-}$ mice result in a lean phenotype, providing protection from diet-induced obesity and insulin resistance (54). This indicates that endogenous MUFA synthesis via SCD1 is an important metabolic control point influencing the cellular decision between energy storage and catabolism. Although some studies have shown SCD1 deficiency to elicit favorable metabolic changes, other studies have also shown that SCD1 activity is protective against the pathophysiological consequences of certain lipotoxicity insults (10, 20, 61). Thus, both excessive and insufficient MUFA synthesis may be causative for disease depending upon the environmental or genetic stimulus.

Since $Scd1^{-/-}$ mice have a reduced capacity for MUFA synthesis, these mice are presumed to have an increased dietary requirement for unsaturated fat. We previously reported that $Scd1^{-/-}$ mice maintained on a very low-fat (VLF) diet for 10 days developed a complex phenotype involving loss of body weight, hypoglycemia, hypercholesterolemia, and cholestasis compared with those fed a standard chow diet (21). $Scd1^{-/-}$ mice are hyperphagic relative to $Scd1^{+/+}$ mice on a chow diet but consume similar amounts of the VLF diet. These phenotypes were largely prevented, independent of food intake, by supplementing the VLF diet with dietary unsaturated fat, but not saturated fat, indicating that reduced endogenous MUFA synthesis, combined with dietary unsaturated fat restriction, elicits a severe metabolic response. Many changes in the VLF $Scd1^{-/-}$ mice were suggestive of altered hepatic metabolism, such as reduced hepatic triglyceride and glycogen, and increased plasma levels of bile acids, bilirubin, and free cholesterol. However, the molecular mechanisms by which this diet-genotype interaction causes hepatic dysfunction are not understood.

In the current study, we performed microarray analysis of hepatic gene expression to explore the metabolic changes responsible for the phenotypes in the VLF $Scd1^{-/-}$ mice. We identified >4,000 differentially expressed probe sets between VLF $Scd1^{-/-}$ mice and both chow-fed $Scd1^{-/-}$ and VLF $Scd1^{+/+}$ mice. Insufficient MUFA synthesis during dietary unsaturated fat restriction results in a dramatic reprogramming of hepatic gene expression, involving decreased expression of lipid metabolism and detoxification genes, decreased abundance of mRNAs encoding key metabolic transcription factors, and a marked increase in the abundance of endoplasmic reticulum (ER) stress and inflammatory response mRNAs. These results highlight an important role of *Scd1* in ER and metabolic homeostasis by maintaining adequate unsaturated fat synthesis during dietary unsaturated fat deficiency.

METHODS

Animals and diets. SV129 $Scd1^{-/-}$ mice were backcrossed to C57BL/6 mice for at least five generations by marker-assisted genotyping. Female C57BL/6 $Scd1^{+/+}$ and $Scd1^{-/-}$ mice were housed in a controlled environment with 12 h light and dark cycles and fed a standard rodent chow diet (PMI 5008 Formulab; PMI Nutrition

Article published online before print. See web site for date of publication (http://physiolgenomics.physiology.org).

Address for reprint requests and other correspondence: M. T. Flowers, Dept. of Biochemistry, Univ. of Wisconsin-Madison, 433 Babcock Dr., Madison, WI 53706 (e-mail: mflowers@biochem.wisc.edu).

International, Richmond, IN) until 12 wk of age. Mice were then randomly assigned to the chow or VLF diet (TD03045; Harlan Teklad, Madison, WI) and fed for an additional 10 days. The VLF diet contains sucrose (49% wt/wt) as the primary carbohydrate source and corn oil (1% wt/wt) as the fat source (21). Protocols for animal experiments were approved by the Animal Care Research Committee of the University of Wisconsin-Madison.

Collection of gene expression data. Mice were fasted for 4 h in the early light cycle and killed by CO_2 asphyxiation. Blood was collected by cardiac puncture, and the liver was subsequently removed and frozen in liquid nitrogen. Total RNA was extracted from liver using RNAzol reagent (Tel-Test) and purified with RNeasy mini columns (Qiagen) before being subjected to microarray studies. Affymetrix Mouse 430 2.0 microarray chips were used to monitor the expression level of 45,101 probe sets representing over 39,000 transcripts and variants from over 34,000 mouse genes (Affymetrix). The complete MIAME formatted data set is deposited as Gene Expression Omnibus accession GSE3889, which may be accessed at http://www.ncbi.nlm.nih.gov/geo. Gene abbreviations are defined in accordance with the Human Gene Nomenclature Committee (9).

Preprocessing and statistical analysis of gene expression data. Expression measurements were preprocessed to provide background correction, normalization, and log base 2 transformation using RMA (robust multiarray average) (33). For each of the four two-group comparisons ($Scd1^{-/-}$ vs. $Scd1^{+/+}$ within each diet and VLF vs. chow diets within each genotype group), we applied both EBarrays (37, 49) and LIMMA (66), each with a false discovery rate of 1%, to ensure that our results are somewhat robust to the statistical method employed. We considered a gene as differentially expressed if it was identified by both methods. RMA, EBarrays, and LIMMA are implemented in R, publicly available statistical analysis environment (62) and available at Bioconductor (24).

EBarrays is an empirical Bayes approach that models the probability distribution of a set of expression measurements (37, 49). It accounts generally for differences among genes in their true underlying expression levels, measurement fluctuations, and distinct expression patterns for a given gene among conditions. An expression pattern is an arrangement of the true underlying intensities (μ) in each condition. The number of patterns possible depends on the number of conditions from which the expression measurements were obtained. For example, when measurements are being compared across pairs of conditions as is the case for this study, two patterns of expression are possible: equivalent expression ($\mu_1 = \mu_2$) and differential expression ($\mu_1 \neq \mu_2$). Since we do not know a priori which genes are in which patterns, the marginal distribution of the data is a mixture over the possible patterns with model parameters determined by the full set of array data. In this way, the approach utilizes information across a set of arrays to optimize model fit and is thus more efficient than a number of methods that make gene inferences one gene at a time. The approach also naturally controls for both type I and type II errors (37). The fitted model parameters provide information on the number of genes expected in each expression pattern. Furthermore, the fitted model is used to assign probability distributions to every gene. Each gene-specific distribution gives the posterior probability of that gene's individual expression pattern. The false discovery rate is controlled by thresholding the posterior probabilities (50).

LIMMA is also a parametric empirical Bayes approach but differs mainly in the form of the posterior odds (or test statistic). In LIMMA, a moderated *t*-statistic is considered where the sample variance is shrunk using information from all genes. With very large sample sizes, the two approaches yield almost identical test statistics, but there are differences with smaller sample sizes (37).

Determination of pathway enrichment. Gene Ontology (GO) biological pathway assignments and pathway enrichment were performed using the NetAffx Gene Ontology Mining Tool (Affymetrix, NetAffx Annotation Release #21, November 2006) (13). Significant pathway enrichment was determined by χ^2 test, and pathways containing at least five probe sets and having a P value <0.05 were considered significantly changed.

Real-time quantitative PCR. Total RNA was reverse transcribed using the iScript cDNA synthesis kit (Bio-Rad). Real-time quantitative PCR was performed on an ABI Prism 7500 Fast instrument using gene-specific primers. Primer sequences may be found in Supplementary Table S1.[1] SYBR green was used for detection and quantification of given genes expressed as mRNA level normalized to 18S ribosomal RNA using the $\Delta\Delta$Ct method (5). We chose 18S ribosomal RNA as a suitable normalization control gene after first evaluating a panel of candidate control genes for similar expression level amongst all samples.

XBP1 splicing assay. Total RNA was reverse transcribed with Invitrogen SuperScript III using oligo(dT) primers. The region of XBP1 containing the splice junction was then amplified by PCR using the XBP1 primers 3S (5′AAACAGAGTAGCAGCGCAGACTGC3′) and 12AS (5′TCCTTCTGGGTAGACCTCTGGGAG3′) with the cycling conditions of 94°C for 5 min, followed by 50 cycles of 94°C for 30 s, 58°C for 30 s, and 72°C for 45 s. The spliced and unspliced PCR products were then digested with *Pst*1, which selectively cleaves unspliced XBP1, and then analyzed on a 2% agarose gel.

Fatty acid composition of hepatic lipids. Total hepatic lipids were extracted according to the method of Bligh and Dyer (8) and analyzed by thin-layer chromatography and gas chromatography, as described previously (16).

RESULTS

Microarray analysis of hepatic gene expression changes in VLF $Scd1^{-/-}$ mice. To better understand the metabolic perturbations elicited by the VLF diet in $Scd1^{-/-}$ mice, we used Affymetrix Mouse 430 2.0 microarray chips to search for gene expression changes unique to the VLF $Scd1^{-/-}$ group. A total of 20 arrays were used to study female $Scd1^{+/+}$ and $Scd1^{-/-}$ mice on chow or the VLF diet (2 strains $\times$ 2 diets $\times$ 5 replicates), giving us the statistical power to detect differentially expressed probe sets with significant fold-changes as low as 1.4 and a false discovery rate of 1%. Table 1 shows the number of increased and decreased probe sets for each diet or genotype comparison. The complete list of probe sets for all four comparisons are available in Supplementary Tables S2–S5. Comparison of the VLF $Scd1^{-/-}$ group to the VLF $Scd1^{+/+}$ and chow $Scd1^{-/-}$ groups revealed 6,593 and 5,124 probe sets, respectively. An intersection of these two comparisons yielded 4,382 shared probe sets, of which 2,728 were increased and 1,654 were decreased. This indicates that the changes are not simply due to a unidirectional shift in the expression profile. The relatively small probe set list for the genotype effect in chow-fed mice and the diet effect in $Scd1^{+/+}$ mice (45 and 158 probe sets, respectively) combined with the lack of disease formation in these groups indicates that the gene expression pattern of the VLF $Scd1^{-/-}$ mice is distinct from the other three groups (21).

To focus on pathways most highly associated with disease progression in the VLF $Scd1^{-/-}$ mice, we analyzed the increased and decreased intersected probe set lists using the NetAffx GO Mining Tool (13). GO Biological Process annotations were available for 1,949 of the 2,728 increased probe sets and 1,123 of the 1,654 decreased probe sets common to both comparisons. The biological pathways that contained at least five probe sets and met our enrichment analysis threshold

[1] The online version of this article contains supplemental material.

Table 1. *Summary of differentially expressed probe sets*

Comparison	Total	Increased	Decreased
VLF: *Scd1*$^{+/+}$ vs. *Scd1*$^{-/-}$	6,593 (2,546)	4,438 (1,752)	2,155 (794)
Chow: *Scd1*$^{+/+}$ vs. *Scd1*$^{-/-}$	45 (12)	40 (8)	5 (4)
Scd1$^{-/-}$: chow vs. VLF	5,124 (2,179)	2,925 (1,276)	2,199 (903)
Scd1$^{+/+}$: chow vs. VLF	158 (69)	103 (43)	55 (26)

Affymetrix Mouse 430 2.0 microarray chips were used to search for hepatic gene expression changes unique to the VLF *Scd1*$^{-/-}$ group. A total of 20 arrays were used to study female *Scd1*$^{+/+}$ and *Scd1*$^{-/-}$ mice on chow or the VLF diet (2 strains × 2 diets × 5 replicates). Lists of differentially expressed probe sets were generated for genotype effects on VLF diet (*row 1*) or chow diet (*row 2*), or for diet effect in *Scd1*$^{-/-}$ mice (*row 3*) or *Scd1*$^{+/+}$mice (*row 4*). For each comparison, the number of total, increased, and decreased probe sets is shown, and those with a fold-change of 2-fold or more are indicated in parentheses. Significant differences were determined as described in METHODS. The complete list of probe sets may be found in the Supplementary Data section. *Scd1*, stearoyl-CoA desaturase 1; *Scd1*$^{+/+}$, wild type; *Scd1*$^{-/-}$, *Scd1* knockout; chow, standard rodent diet; VLF, very low fat diet.

of $P < 0.05$ are summarized in Supplementary Tables S6 and S7. The pathway enrichment analysis revealed a striking downregulation of genes involved in many metabolic pathways. Most notably, we observed a high enrichment of lipid metabolism genes with decreased expression involved in both fatty acid and steroid metabolism. Changes related to fatty acid metabolism are described in detail below. Interestingly, analysis of both the increased and decreased probe set lists identified amino acid metabolism as an enriched pathway, affecting both amino acid biosynthesis and catabolism genes. Our analysis of both the increased and decreased probe set lists also identified pathway enrichment for genes involved in transcription, including alterations in the mRNA abundance of key metabolism transcription factors. Among genes with increased expression, there was an enrichment of those related to the cellular response to various stimuli (stress, defense, biotic, abiotic, chemical, and external). In particular, we observed a marked increase in the expression of ER stress and inflammation genes in the VLF *Scd1*$^{-/-}$ mice, which we suggest is responsible for the metabolic alterations presented in the next section and summarized in Fig. 1.

Fatty acid synthesis, elongation, and desaturation. *Scd1*$^{-/-}$ mice have previously been shown to have impaired upregulation of genes involved in fatty acid and triglyceride synthesis in response to high-carbohydrate feeding (46, 48). As shown in Table 2, VLF *Scd1*$^{-/-}$ mice showed either no upregulation or even a downregulation (relative to chow diet levels) of several lipogenic genes including *Pklr* (liver pyruvate kinase), *Acly* (ATP citrate lyase), *Acas2* (acetyl-CoA synthetase 2), *Acaca* (ACCα), *Acacb* (ACCβ), *Fasn* [fatty acid synthase (FAS)], *Mod1* (malic enzyme), *Thrsp* (SPOT14), *Gpam* (mitochondrial glycerol-3-phosphate acyltransferase), and *Dgat2* (diacylglycerol-O-acyltransferase 2). The expression of several hepatic fatty acid elongases (*Elovl2*, *Elovl5,* and *Elovl6*) as well as the Δ5 desaturase *Fads1* and Δ6 desaturase *Fads2* also decreased or failed to increase, while *Elovl1* and *Scd2* (Δ9) were increased. The MUFA synthesis derived from *Scd2*, which is a minor hepatic SCD isoform in the mouse, is apparently insufficient to make up for the lack of *Scd1* in VLF *Scd1*$^{-/-}$ mice. In the context of the 10-day VLF feeding regimen, this gene expression pattern indicates that *Scd1*$^{-/-}$ mice fail to compensate for the limited availability of dietary unsaturated fatty acids, whereas *Scd1*$^{+/+}$ mice maintain unsaturated fatty acid homeostasis by increasing the hepatic synthesis of fatty acids from carbohydrate and other lipogenic precursors.

We also analyzed the fatty acid composition of total hepatic lipids in all four groups. When fed the VLF diet, *Scd1*$^{+/+}$ mice respond by increasing the hepatic content of the MUFA palmitoleic acid (16:1), oleic acid (18:1, n9) and vaccenic acid (18:1, n7) (Fig. 2). As expected, *Scd1* deficiency on both the chow and VLF diets reduced the hepatic content of 16:1, 18:1n9, and 18:1n7. VLF feeding also reduced the hepatic content of the polyunsaturated fatty acids linoleic acid (18:2, n6) and docosahexaenoic acid (22:6, n3) in both *Scd1*$^{+/+}$ and *Scd1*$^{-/-}$ mice, and the content of arachidonic acid (20:4, n6) in *Scd1*$^{-/-}$ mice. Since the Δ9-desaturase system is the only source of de novo unsaturated fat in mammals, *Scd1*-deficient mice fed the VLF diet have limited unsaturated fat available from the diet or endogenous synthesis.

Fatty acid oxidation, ketogenesis, and lipid transport. In addition to fatty acid synthesis genes, those involved in several other facets of fatty acid metabolism were found to be differentially expressed between VLF *Scd1*$^{-/-}$ mice and control groups. This list includes genes involved in mitochondrial fatty acid transport (*Cpt1a*, *Cpt2*, *Mlycd*), peroxisomal fatty acid transport (*Slc27a2*, *Abcd2*, *Abcd3*), fatty acid oxidation (*Acox1*, *Crot, Acox2*), and ketogenesis (*Hmgcs2*, *Aacs*, *Bdh*) (Table 2). An alteration in fatty acid oxidation gene expression is further

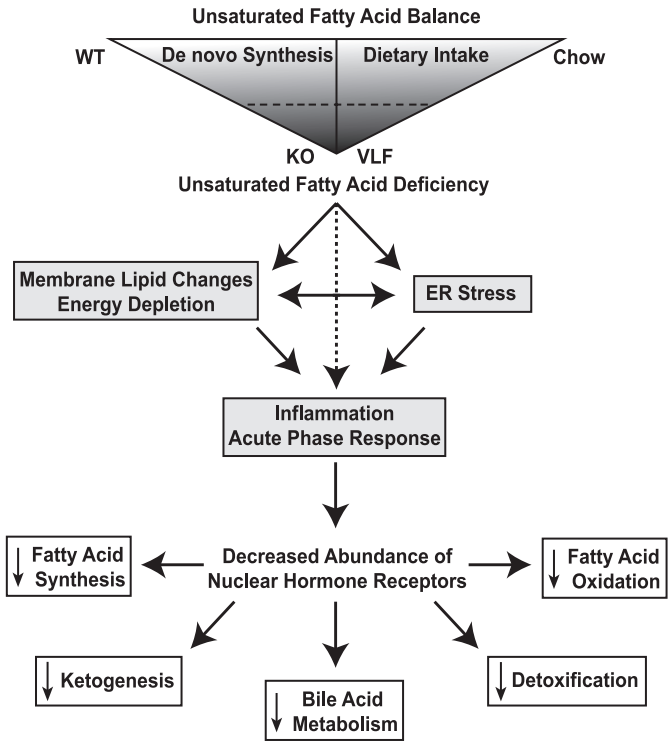

Fig. 1. Metabolic dysfunction mediated through unsaturated fatty acid deficiency and ER stress. Whole body unsaturated fatty acid balance is maintained by de novo synthesis and dietary intake, both of which are limited in VLF *Scd1*$^{-/-}$ mice causing unsaturated fatty acid deficiency (indicated by the apex of the triangle). This elicits an ER stress and inflammatory response that leads to a decreased mRNA abundance of nuclear hormone receptors that control the expression level of genes involved in several facets of metabolism. VLF, very low fat-fed; ER, endoplasmic reticulum; WT, wild type; KO, knockout; *Scd1*, stearoyl-CoA desaturase 1.

Table 2. *Fatty acid metabolism*

Probe Set ID	Gene Symbol	Gene Name	Chow		VLF	
			Scd1$^{+/+}$	*Scd1*$^{-/-}$	*Scd1*$^{+/+}$	*Scd1*$^{-/-}$
		Fatty Acid Synthesis				
1421258_a_at	*Pklr*	Liver pyruvate kinase	1.00	1.29	2.72†	0.95*
1451666_at	*Acly*	ATP-citrate lyase	1.00	1.03	2.29	0.87*
1422479_at	*Acas2*	Acetyl-CoA synthase 2	1.00	0.80	2.84	0.73*
1434185_at	*Acaca*	Acetyl-CoA carboxylase 1	1.00	1.01	3.11†	0.69*
1427052_at	*Acacb*	Acetyl-CoA carboxylase 2	1.00	1.04	2.38†	0.65*
1423828_at	*Fasn*	Fatty acid synthase	1.00	1.01	3.52†	0.38*†
1430307_a_at	*Mod1*	Malic enzyme	1.00	0.94	2.81	0.68*
1424737_at	*Thrsp*	Spot 14	1.00	1.74	2.83	0.38*†
1419499_at	*Gpam*	Glycerol-3-P acyltransferase (m)	1.00	1.02	1.49	0.82*
1422678_at	*Dgat2*	Diacylglycerol O-acyltransferase 2	1.00	1.02	1.11	0.35*†
		Elongation and Desaturation				
1456530_x_at	*Elovl1*	Elongation of VLCFA 1	1.00	1.02	1.16	2.01*†
1416444_at	*Elovl2*	Elongation of VLCFA 2	1.00	0.85	1.48	0.50*†
1437211_x_at	*Elovl5*	Elongation of VLCFA 5	1.00	0.82	1.96†	0.79*
1417404_at	*Elovl6*	Elongation of VLCFA 6	1.00	1.13	5.67†	0.38*†
1423680_at	*Fads1*	Fatty acid desaturase 1 (Δ5)	1.00	0.83	1.62†	0.38*†
1419031_at	*Fads2*	Fatty acid desaturase 1 (Δ6)	1.00	0.88	2.03†	0.49*†
1415965_at	*Scd1*	Stearoyl-CoA desaturase 1 (Δ9)	1.00	0.03*	6.46†	0.03*
1415822_at	*Scd2*	Stearoyl-CoA desaturase 2 (Δ9)	1.00	1.20	1.54	5.75*†
		Oxidation and Ketogenesis				
1460409_at	*Cpt1a*	Carnitine palmitoyltransferase 1a	1.00	1.29	1.33	0.85*
1416772_at	*Cpt2*	Carnitine palmitoyltransferase 2	1.00	0.99	1.02	0.62*†
1449964_a_at	*Mlycd*	Malonyl-CoA decarboxylase	1.00	0.97	0.90	0.56*†
1416316_at	*Slc27a2*	Very long-chain acyl-CoA dehydrogenase synthase	1.00	1.12	0.99	0.37*†
1456812_at	*Abcd2*	ATP-binding cassette, subfamily D (ALD), member 2	1.00	0.94	0.87	0.22*†
1416679_at	*Abcd3*	ATP-binding cassette, subfamily D (ALD), member 3	1.00	0.97	1.11	0.52*†
1416408_at	*Acox1*	Palmitoyl-CoA oxidase 1	1.00	1.09	1.00	0.47*†
1420673_a_at	*Acox2*	Branched chain Acyl-CoA oxidase 2	1.00	1.17	0.78	1.30*
1450966_at	*Crot*	Carnitine O-octanoyltransferase	1.00	0.98	0.62	0.29*†
1423858_a_at	*Hmgcs2*	HMG-CoA synthase 2	1.00	1.10	1.07	0.51*†
1456081_a_at	*Aacs*	Acetoacetyl-CoA synthetase	1.00	1.45	2.08†	0.77*
1452257_at	*Bdh*	3-Hydroxybutyrate dehydrogenase	1.00	1.08	1.17	0.46*†

Changes in gene expression are reported as ratios relative to chow-fed *Scd1*$^{+/+}$ mice. Significant differences were determined as described in METHODS. *Genotype effect; †diet effect.

exemplified by the reduced expression of several acyl-CoA dehydrogenases, enoyl-CoA hydratases, enoyl-CoA reductases, 3-oxoacyl CoA-thiolases, and dodecenoyl-CoA delta isomerase, as well as an increase and decrease in mitochondrial and peroxisomal thioesterases, respectively (Supplementary Tables S2 and S4). VLF *Scd1*$^{-/-}$ mice also showed altered expression of lipid transport genes for several acyl-CoA synthetases (*Acsl1*, *Acsl4*), fatty acid and acyl-CoA binding proteins (*Dbi*, *Fabp1*, *Scp2*), lipases (*Lipc*, *Lipg*, *Mgll*, *Lpl*), and the lipoprotein lipase (*Lpl*) inhibitor *Angptl3* (Table 3). Interestingly, the transcript level of *Lpl*, which is normally not expressed in the adult liver, was highly elevated in VLF *Scd1*$^{-/-}$ mice (45).

Hepatic carbohydrate metabolism. We previously observed severe hypoglycemia in the VLF *Scd1*$^{-/-}$ mice despite being maintained on the carbohydrate-rich VLF diet (21). This hypoglycemia could potentially be due to increased hepatic glucose uptake and/or decreased gluconeogenesis. As shown in Table 3, we observed only a slight decrease in the expression of the major hepatic glucose transporter *Slc2a2* (Glut2) and fructose transporter *Slc2a5* (Glut5). The entry of glucose and fructose into glycolysis requires phosphorylation by glucokinase (*Gck*) and fructokinase (*Khk*). *Gck* was downregulated, while *Khk* failed to increase to wild-type levels in response to the VLF diet. We also observed a large increase in the mRNA expression of the glucose transporter *Slc2a1* (Glut1) and *Pdk4* (pyruvate dehydrogenase kinase 4), which are both elevated during starvation and glucose deprivation (67, 69). We observed suppression of the gluconeogenic gene *Fbp1* (fructose-1,6-bisphosphatase 1) and a lesser effect on *Pcx* (pyruvate carboxylase) (Table 3).

VLF Scd1$^{-/-}$ *mice have altered abundance of key metabolic transcription factors.* One mechanism for the broad reprogramming of hepatic gene expression in the VLF *Scd1*$^{-/-}$ mice is the unexpected change in transcription factor mRNA abundance (Table 4). The VLF *Scd1*$^{-/-}$ mice have decreased hepatic expression of the major lipogenic transcription factors *Srebf1* (SREBP1), *Wbscr14* (ChREBP), and *Nr1h3* (LXRα). Reduced expression of *Ppara* (PPARα) may be responsible for the altered fatty acid metabolism gene expression (Tables 2 and 3). Several key hepatic transcription factors and coactivators important for gluconeogenesis were altered, including reduced expression of *Hnf4a* (HNF4α), *Nr3c1* (glucocorticoid receptor), and *Cebpa* (C/EBPα), but increased expression of *Ppargc1a* (PGC1α), *Nr4a1* (Nur77), and *Nr4a2* (Nurr1) (56, 60, 63, 74). We previously found marked suppression of genes

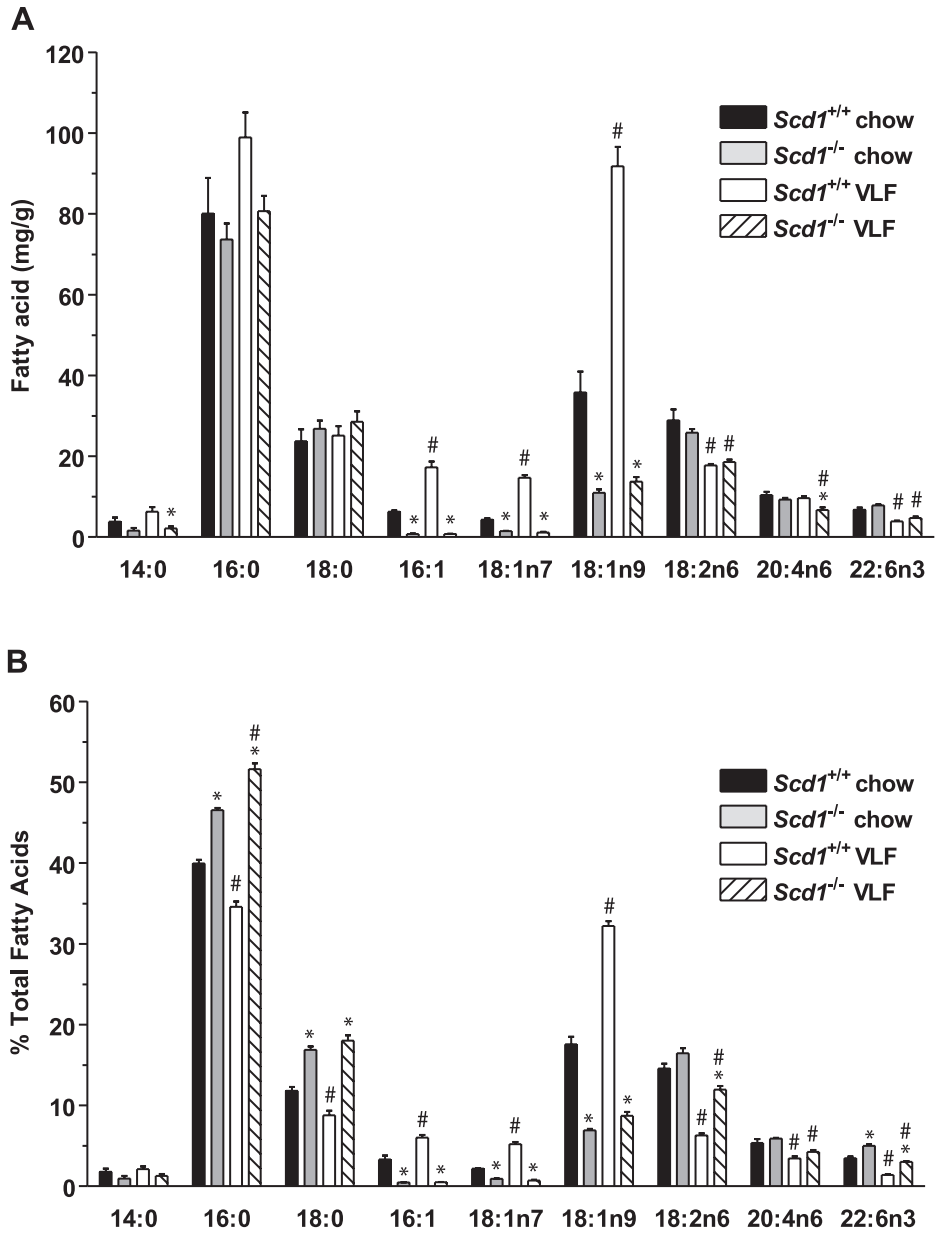

Fig. 2. Fatty acid composition of total hepatic lipids. Fatty acid composition of total hepatic lipids of *Scd1*$^{+/+}$ and *Scd1*$^{-/-}$ mice on chow or the VLF diet. Results are expressed as means ± SE for 5–7 mice per group. *A*: fatty acid mass (mg/g liver). *B*: percent of total fatty acids. *Genotype effect (within same diet); #diet effect (within same genotype). Data were analyzed by 2-way ANOVA with Bonferroni's posttest and considered significant when $P < 0.05$.

involved in bile acid metabolism and transport (21), which is likely related to the decreased expression of *Nr1h4* (FXR), *Nr5a2* (LRH-1), and *Nr2f2* (COUP-TF2) (15). A more widespread effect on gene expression is predicted by the decreased expression of the coactivator *Ppargc1b* (PGC1β) and the type II nuclear hormone receptor dimerization partner *Rxra* (RXRα) (19, 70). Additionally, increased expression of the transcriptional repressors *Nrip1* (RIP140) and *Cri1* (Eid1) may act to further antagonize nuclear receptor-dependent gene transcription (6, 59).

Another subset of transcription factors showing reduced expression were those involved in regulating detoxification and drug metabolism enzymes, including *Hlf* (hepatic leukemia factor), *Tef* (thyrotroph embryonic factor), *Dbp* (D site albumin promoter binding protein), and *Nr1i3* (CAR) (Table 4) (22). Consistent with the reduced expression of detoxification genes observed in *Hlf/Tlf/Dbp* triple knockout mice (22), we observed decreased expression of many carboxylesterases (*Ces1, Ces3, Ces6, Es22)*, sulfotransferases (*Sult1b1, Sult1c2, Sult2a2, Sult3a1, Sult5a1),* carbonic anhydrases (*Car1, Car3, Car5a, Car8*), aldehyde dehydrogenases (*Aldh2, Aldh1b1, Aldh4a1-Aldh9a1*), and UDP-glucuronosyltransferases (*Ugt1a6, Ugt2b5, Ugt3a1, Ugt3a2*), as well as differential expression of many cytochrome P450 genes and glutathione-S-transferase genes (Supplementary Tables S2 and S4). It is important to note that for some of these genes, the *Scd1*$^{+/+}$ mice showed an intermediary response to the VLF diet relative to *Scd1*$^{-/-}$ mice (Supplementary Tables S2–S5). Although the majority of the gene expression changes in this group suggest impaired detoxification, some members of these gene clusters were increased in the VLF *Scd1*$^{-/-}$ mice. Interestingly, the expression of several targets of the oxidative stress-activated transcription factor *Nfe2l2* (Nrf2) were increased in VLF *Scd1*$^{-/-}$ mice, including *Akr1b3* (aldose reductase), *Hmox1* (heme oxygenase 1), and

Table 3. *Lipid transport and carbohydrate metabolism*

Probe Set ID	Gene Symbol	Gene Name	Chow		VLF	
			Scd1$^{+/+}$	*Scd1*$^{-/-}$	*Scd1*$^{+/+}$	*Scd1*$^{-/-}$
		Lipid Transport				
1423883_at	*Acsl1*	Acyl-CoA synthetase 1	1.00	0.94	0.92	0.32*†
1433531_at	*Acsl4*	Acyl-CoA synthetase 4	1.00	1.85	1.81	5.15*†
1455976_x_at	*Dbi*	Diazepam binding inhibitor	1.00	0.86	1.11	0.71*
1417556_at	*Fabp1*	Liver fatty acid binding protein 1	1.00	0.97	1.07	0.38*†
1426219_at	*Scp2*	Sterol carrier protein 2	1.00	0.92	1.01	0.56*†
1419560_at	*Lipc*	Hepatic lipase	1.00	0.98	0.89	0.19*†
1421262_at	*Lipg*	Endothelial lipase	1.00	1.90	1.42	0.41*†
1426785_s_at	*Mgll*	Monoglyceride lipase	1.00	0.90	1.38	0.38*†
1415904_at	*Lpl*	Lipoprotein lipase	1.00	1.22	0.84	12.52*†
1424485_at	*Angptl3*	Angiopoietin-like 3	1.00	0.90	1.03	0.52*†
		Carbohydrate Metabolism				
1434773_a_at	*Slc2a1*	Glut 1	1.00	1.65	1.45	7.35*†
1449067_at	*Slc2a2*	Glut 2	1.00	1.37	1.22	0.85†
1416639_at	*Slc2a5*	Glut 5	1.00	1.12	1.15	0.75*†
1425303_at	*Gck*	Glucokinase	1.00	0.95	1.39	0.56*†
1449062_at	*Khk*	Fructokinase	1.00	1.27	1.89†	1.23*
1455209_at	*Pck1*[1]	PEPCK (c)[1]	1.00	1.01	0.81	0.30*†[1]
1448470_at	*Fbp1*	Fructose-1,6-bisphosphatase 1	1.00	1.02	1.04	0.57*†
09192_MB_at	*Pcx*	Pyruvate carboxylase	1.00	1.39	1.40	0.90*†
1417273_at	*Pdk4*	Pyruvate dehydrogenase kinase 4	1.00	1.32	1.28	14.73*†

Changes in gene expression are reported as ratios relative to chow-fed *Scd1*$^{+/+}$ mice. Significant differences were determined as described in METHODS. *Genotype effect; †diet effect. [1]Note: *Pck1* was not confirmed to be differentially expressed by real-time PCR (see Fig. 3*A*).

Nqo1 [NAD(P)H:quinine oxidoreductase 1], which may explain the increased expression of genes encoding some detoxification and antioxidant enzymes (Table 5) (38, 51).

Integrated stress response. Nutrient deprivation, ER stress, and oxidative stress elicit an integrated stress response pathway that induces a transcriptional program to help cope with and resolve cell stress. In the VLF *Scd1*$^{-/-}$ mice, the eIF2α kinase *Eif2ak3* (PERK), as well as the stress-activated transcription factors *Atf4* and *Atf6* were all increased (Table 5). However, these targets are not typically regulated at the transcriptional level (27, 29). More importantly, several transcriptional targets of ATF4 and ATF6 activation were induced, including the transcription factors *Atf3* and *Ddit3* (CHOP), as well as the chaperones *Hspa5* (GRP78/BiP) and *Hsp90b1* (GRP94/TRA1) (34). Prolonged induction of ER stress is indicated by the increased expression of *Trib3*, which acts as a transcriptional repressor to attenuate CHOP- and ATF4-mediated transcription (35, 55). Further hepatic stress is evidenced by elevated

Table 4. *Transcription factors*

Transcription Factors			Chow		VLF	
Probe Set ID	Gene Symbol	Gene Name	*Scd1*$^{+/+}$	*Scd1*$^{-/-}$	*Scd1*$^{+/+}$	*Scd1*$^{-/-}$
1426690_a_at	*Srebf1*	SREBP-1	1.00	1.00	1.55	0.44*†
1419185_a_at	*Wbscr14*	ChREBP	1.00	0.88	0.96	0.33*†
1450444_a_at	*Nr1 h3*	LXRα	1.00	1.07	1.03	0.69*†
1449051_at	*Ppara*	PPARα	1.00	1.14	1.29	0.48*†
1450447_at	*Hnf4a*	HNF4α	1.00	1.17	1.10	0.76*†
1421867_at	*Nr3c1*	Glucocorticoid receptor	1.00	0.94	0.94	0.57*†
1418982_at	*Cebpa*	C/EBP alpha	1.00	0.94	1.10	0.29*†
1456395_at	*Ppargc1a*	PGC-1α	1.00	1.24	1.02	3.54*†
1416505_at	*Nr4a1*	Nur77	1.00	0.94	0.94	2.85*†
1450750_a_at	*Nr4a2*	Nurr1	1.00	0.85	0.90	1.81*†
1419105_at	*Nr1 h4*	FXR	1.00	1.11	0.93	0.41*†
1449706_s_at	*Nr5a2*	LRH-1	1.00	1.07	1.06	0.65*†
1416158_at	*Nr2f2*	COUP-TF2	1.00	1.27	1.09	0.68*†
1449945_at	*Ppargc1b*	PGC-1β	1.00	1.09	0.92	0.46*†
1454773_at	*Rxra*	RXRα	1.00	1.16	0.99	0.63*†
1449089_at	*Nrip1*	RIP140	1.00	1.03	0.92	2.16*†
1416614_at	*Cri1*	Eid1	1.00	1.30	1.01	2.30*†
1434736_at	*Hlf*	Hepatic leukemia factor	1.00	1.28	1.40	0.68*†
1424175_at	*Tef*	Thyrotroph embryonic factor	1.00	1.21	1.18	0.53*†
1438211_s_at	*Dbp*	D site albumin promoter binding protein	1.00	1.49	1.78	0.19*†
1425392_a_at	*Nr1i3*	CAR	1.00	1.23	0.83	0.31*†

Changes in gene expression are reported as ratios relative to chow-fed *Scd1*$^{+/+}$ mice. Significant differences were determined as described in METHODS. *Genotype effect; †diet effect.

Table 5. *Stress response*

Stress Response			Chow		VLF	
Probe Set ID	Gene Symbol	Gene Name	*Scd1*$^{+/+}$	*Scd1*$^{-/-}$	*Scd1*$^{+/+}$	*Scd1*$^{-/-}$
1449278_at	*Eif2ak3*	Eukaryotic translation initiation factor 2 alpha kinase 3 (PERK)	1.00	1.25	0.94	3.35*†
1449363_at	*Atf3*	Activating transcription factor 3	1.00	0.91	1.00	13.66*†
1448135_at	*Atf4*	Activating transcription factor 4	1.00	1.06	0.86	1.51*
1453288_at	*Atf6*	Activating transcription factor 6	1.00	1.27	1.01	2.66*†
1417516_at	*Ddit3*	GADD153 (CHOP)	1.00	0.86	0.89	9.68*†
1426065_a_at	*Trib3*	Tribbles homolog 3 (*Drosophila*)	1.00	1.28	0.82	2.10*†
1448325_at	*Myd116*	Myeloid differentiation primary response gene 116 (GADD34)	1.00	1.03	0.79	3.39*†
1416064_a_at	*Hspa5*	Heat shock 70 kDa protein 5 (BiP/Grp78)	1.00	1.31	1.28	3.08*†
1438040_a_at	*Hsp90b1*	Heat shock protein 90 kDa beta (Grp94), member 1	1.00	1.58	1.31	3.02*†
1452388_at	*Hspa1a*	Heat shock protein 1A (Hsp70.3)	1.00	0.97	0.92	17.92*†
1452318_a_at	*Hspa1b*	Heat shock protein 1B (Hsp70.1)	1.00	1.64*	1.66	12.38*†
1425964_x_at	*Hspb1*	Heat shock protein 1 (Hsp25)	1.00	0.76	0.49	2.01*†
1426645_at	*Hspca*	Heat shock protein 90 kDa alpha (cytosolic), class A member 1	1.00	1.19	1.38	2.60*†
1418918_at	*Igfbp1*	Insulin-like growth factor binding protein 1	1.00	4.15	1.18	13.91*†
1451095_at	*Asns*	Asparagine synthetase	1.00	2.23	1.02	8.50*†
1454991_at	*Slc7a1*	Solute carrier family 7 (CAT-1)	1.00	0.82	0.95	2.51*†
1423627_at	*Nqo1*	NADPH dehydrogenase/quinone 1	1.00	1.25	1.25	5.88*†
1437133_x_at	*Akr1b3*	Aldo-keto reductase family 1/member B3 (aldose reductase)	1.00	1.18	0.97	7.73*†
1448239_at	*Hmox1*	Heme oxygenase (decycling) 1	1.00	1.19	0.86	4.10*†
1417962_s_at	*Ghr*	Growth hormone receptor	1.00	1.01	0.96	0.19*†
1452014_a_at	*Igf1*	Insulin-like growth factor 1	1.00	0.90	0.81	0.27*†
1423691_x_at	*Krt8*	Keratin complex 2/basic/gene 8	1.00	1.12	0.78	6.98*†
1448169_at	*Krt18*	Keratin complex 1/acidic/gene 18	1.00	1.04	0.83	4.70*†

Changes in gene expression are reported as ratios relative to chow-fed *Scd1*$^{+/+}$ mice. Significant differences were determined as described in METHODS. *Genotype effect; †diet effect.

expression of the ATF4 target *Igfbp1* as well as several stress-induced chaperones including *Hspa1a, Hspa1b, Hspb1,* and *Hspca* (32, 44). Together, this strongly suggests that the combined deficiency of dietary and de novo synthesized unsaturated fatty acids is either directly (via changes in fatty acid availability or composition) or indirectly (via impaired energy production) activating the integrated stress response pathway.

ER stress is often associated with elevated phosphorylation of eIF2α, which inhibits general protein synthesis but increases translation of ATF4 (36). Subsequently, ATF4 transcriptionally activates genes involved in amino acid metabolism that may protect against oxidative stress by promoting glutathione synthesis (28). We observed increased expression of two well-established markers of this amino acid response, the amino acid transporter *Slc7a1* (CAT1) (17) and the amino acid biosynthetic enzyme *Asns* (asparagine synthetase) (2), as well as several aminoacyl tRNA synthetases (Table 5 and Supplementary Tables S2 and S4). Amino acid catabolism genes were also decreased, including ornithine transcarbamylase (*Otc*), branched chain aminotransferase 2 (*Bcat2*), proline dehydrogenase (*Prodh* and *Prodh2*), tryptophan 2,3-dioxygenase (*Tdo2*), and 4-hydroxyphenylpyruvate dioxygenase (*Hpd*) (Supplementary Tables S2 and S4). Decreased amino acid catabolism has been shown to decrease the availability of gluconeogenic substrates and may contribute to hypoglycemia in VLF *Scd1*$^{-/-}$ mice (26).

Although we observed enhanced phosphorylation of eIF2α in positive control samples treated with tunicamycin, this was not seen in VLF *Scd1*$^{-/-}$ mice (data not shown). We speculate that the 10-day VLF feeding of *Scd1*$^{-/-}$ mice leads to an adaptation to prolonged ER stress, as evidenced by increased expression of *Gadd34/Myd116*, which promotes the dephosphorylation of eIF2α to promote recovery from translational inhibition during the unfolded protein response (Table 5) (52).

Inflammation and macrophage infiltration. Hepatic inflammation and necrosis were evident in histological sections from VLF *Scd1*$^{-/-}$ livers, which showed an abnormal hepatocytic appearance, characterized by marked cellular infiltration, cellular swelling, prominent Kupffer cells, multifocal areas of mixed inflammatory cells, and necrotic cellular debris (Supplementary Fig. S1). This observation is supported by the elevated expression of macrophage recruitment and liver inflammation genes such as cellular adhesion molecules (*Icam1, Vcam1*), matrix metalloproteases (*Mmp12, Mmp13, Mmp14, Adamts1*), macrophage cell surface glycoproteins (*Cd14, Cd38, Cd68, Emr1*), cytokines (*Ccl2, Ccl6, Cxcl2, Cxcl4, Cxcl10, Cxcl16, Tgfb1*), and cytokine receptors (*Cxcr4, Csf1r, Ccr1, Ccrl1, Ccrl2, Ifngr1, Tlr2)* (Table 6 and Supplementary Tables S2 and S4). We also observed increased expression of the protooncogenes *Myc, Jun,* and *Fos,* as well as a dramatic induction of *Afp* (alpha-fetoprotein) and *Lcn2* (lipocalin 2), all of which have been shown to increase in response to inflammation (Table 6) (7, 72). This inflammatory response is further indicated by the decreased expression of many hepatic-negative acute-phase mRNAs, including *Prlr* (prolactin receptor), *Dio1* (type I iodothyronine deiodinase), and major urinary proteins *Mup1*, *Mup3*, and *Mup5* (14, 25, 75).

Real-time PCR confirmation and evidence of ER stress activation. Using real-time PCR, we verified the differential expression of 23 key genes from the microarray experiment (Fig. 3, *A–D*). However, while *Pck1* (cytosolic phosphoenolcarboxykinase) was found to be differentially expressed by one probe set on the microarray (Table 3), this finding could not be replicated by real-time PCR (Fig. 3*A*). The presence of ER stress in VLF *Scd1*$^{-/-}$ mice is further indicated by the increased abundance of spliced XBP1 mRNA (Fig. 3*E*), which is derived from the inositol-requiring enzyme 1 (IRE1)-dependent cleavage of XBP1 mRNA in response to unfolded proteins

Table 6. *Inflammatory and acute phase response*

Inflammatory and Acute Phase Response			Chow		VLF	
Probe Set ID	Gene Symbol	Gene Name	*Scd1*$^{+/+}$	*Scd1*$^{-/-}$	*Scd1*$^{+/+}$	*Scd1*$^{-/-}$
1424067_at	*Icam1*	Intercellular adhesion molecule	1.00	1.13	0.89	2.64*†
1448162_at	*Vcam1*	Vascular cell adhesion molecule 1	1.00	2.21	1.03	8.00*†
1449153_at	*Mmp12*	Matrix metalloproteinase 12	1.00	0.87	0.98	19.93*†
1417256_at	*Mmp13*	Matrix metalloproteinase 13	1.00	1.01	0.98	5.02*†
1416572_at	*Mmp14*	Matrix metalloproteinase 14	1.00	1.38	1.17	3.43*†
1450716_at	*Adamts1*	ADAM metalloprotease with thrombospondin type 1 motif, 1	1.00	1.04	1.04	2.28*†
1417268_at	*Cd14*	CD14 antigen	1.00	1.18	0.95	36.44*†
1433741_at	*Cd38*	CD38 antigen	1.00	1.34	1.05	2.11*†
1449164_at	*Cd68*	CD68 antigen	1.00	1.41	1.14	6.26*†
1451161_a_at	*Emr1*	Cell surface glycoprotein F4/80; lymphocyte antigen 71	1.00	1.00	0.78	1.52*†
1424942_a_at	*Myc*	Myelocytomatosis oncogene	1.00	0.90	0.76	4.13*†
1417409_at	*Jun*	Jun oncogene	1.00	1.65	0.94	4.71*†
1423100_at	*Fos*	FBJ osteosarcoma oncogene	1.00	1.75	1.05	9.13*†
1416646_at	*Afp*	Alpha fetoprotein	1.00	0.94	0.97	24.61*†
1427747_a_at	*Lcn2*	Lipocalin 2	1.00	10.67	1.02	61.12*†
1421382_at	*Prlr*	Prolactin receptor	1.00	0.95	0.72	0.14*†
1417991_at	*Dio1*	Deiodinase/iodothyronine/type I	1.00	1.11	0.92	0.06*†
1434110_x_at	*Mup1*	Major urinary protein 1	1.00	1.20	0.80	0.11*†
1427631_x_at	*Mup3*	Major urinary protein 3	1.00	1.02	0.85	0.15*†
1426166_at	*Mup5*	Major urinary protein 5	1.00	1.06	0.91	0.32*†

Changes in gene expression are reported as ratios relative to chow-fed *Scd1*$^{+/+}$ mice. Significant differences were determined as described in METHODS. *Genotype effect; †diet effect. Several cytokines and cytokine receptors were differentially expressed and may be found in the Supplementary Data section.

and encodes a transcription factor involved in the ER stress response (36). Overall, this gene expression profile indicates that a 10-day restriction of dietary unsaturated fatty acids in *Scd1*$^{-/-}$ mice causes abnormal lipid metabolism, promotes a severe state of hepatic ER stress and inflammation, and is associated with an alteration in the abundance of key metabolic transcription factors.

DISCUSSION

We previously established an in vivo model to explore the physiological consequences of combined dietary and de novo unsaturated fat deficiency by feeding *Scd1*$^{-/-}$ mice a VLF diet for 10 days (21). These mice developed several markers of hepatic dysfunction, including hypoglycemia, hypercholesterolemia, and elevated levels of plasma bile acids, bilirubin, and aminotransferases, which we proposed to be due to alterations in membrane lipid composition affecting canalicular membrane function and causing cholestasis. To further delineate the mechanisms contributing to these phenotypes in the VLF *Scd1*$^{-/-}$ mice, we performed microarray analysis of hepatic gene expression. The gene expression profiling in the current study reveals a complex network of changes unique to the VLF *Scd1*$^{-/-}$ mice that highlight the involvement of cellular stress and inflammatory responses associated with the hepatic dysfunction in this model.

Although an extrahepatic physical obstruction or an intrahepatic disorder of the bile ducts can impede bile flow, several other insults can also cause cholestasis at the hepatocellular level, such as bacterial infection, sepsis, pregnancy, ischemia, and response to drugs, toxins, and viruses (23). This commonly occurs via modulation of the expression level or localization of several hepatic sinusoidal and canalicular organic anion transporters via inflammatory cytokines, endotoxins, hormones, bile acids, and oxidative stress (23, 65). Consistent with other models of cholestasis in rodents, VLF *Scd1*$^{-/-}$ mice show altered expression of several organic anion transporters, decreased expression of *Ghr* (growth hormone receptor) and *Igf1* (insulin-like growth factor 1), and increased expression of the cytokeratins *Krt8* and *Krt18* (Table 5) (18, 21, 30). The marked elevation of serum alanine and aspartate aminotransferases but modest elevation of alkaline phosphatase in VLF *Scd1*$^{-/-}$ mice is suggestive of acute hepatitis, rather than an obstructive origin of cholestasis (1, 21). The intracellular accumulation of hepatic organic anions is itself a cellular stressor, but microarray analysis of bile duct-ligated female mice revealed only a relatively modest alteration in the gene expression profile (<150 genes with at least a twofold change) (11). Thus, the gene expression profile of the VLF *Scd1*$^{-/-}$ mice suggests that a large number of hepatic responses are occurring independently of those due to hepatic accumulation of organic anions in obstructive cholestasis.

While the current study is limited to the liver, it is likely that other tissues are involved in the phenotypes of the VLF *Scd1*$^{-/-}$ mice. For example, liver-derived lipoprotein lipids can influence the fatty acid composition of adipose tissue, and adipose-derived free fatty acids are taken up by the liver. Effects of unsaturated fatty acid depletion in extrahepatic tissues may also indirectly influence the liver via changes in hormones or metabolic flux. Therefore, it is difficult to isolate the direct hepatic effects with the VLF whole body *Scd1*$^{-/-}$ mouse model. We have recently reported on phenotypes of the liver-specific *Scd1*-deficient mice fed the VLF diet (47). These mice recapitulate a subset of the metabolic phenotypes observed in the VLF whole body *Scd1*$^{-/-}$ mice, such as loss of body weight, hypoglycemia, reduced liver glycogen, and decreased liver and plasma triglycerides, but do not develop the cholestasis-like phenotypes of elevated plasma bile acids, bilirubin, and lipoprotein-X (unpublished data and Ref. 47). This indicates that loss of *Scd1* in extrahepatic tissues influences the severity of the VLF-induced hepatic dysfunction.

Connection of SCD1 to the integrated stress response. Recently, pharmacological inhibition of FAS was shown to induce

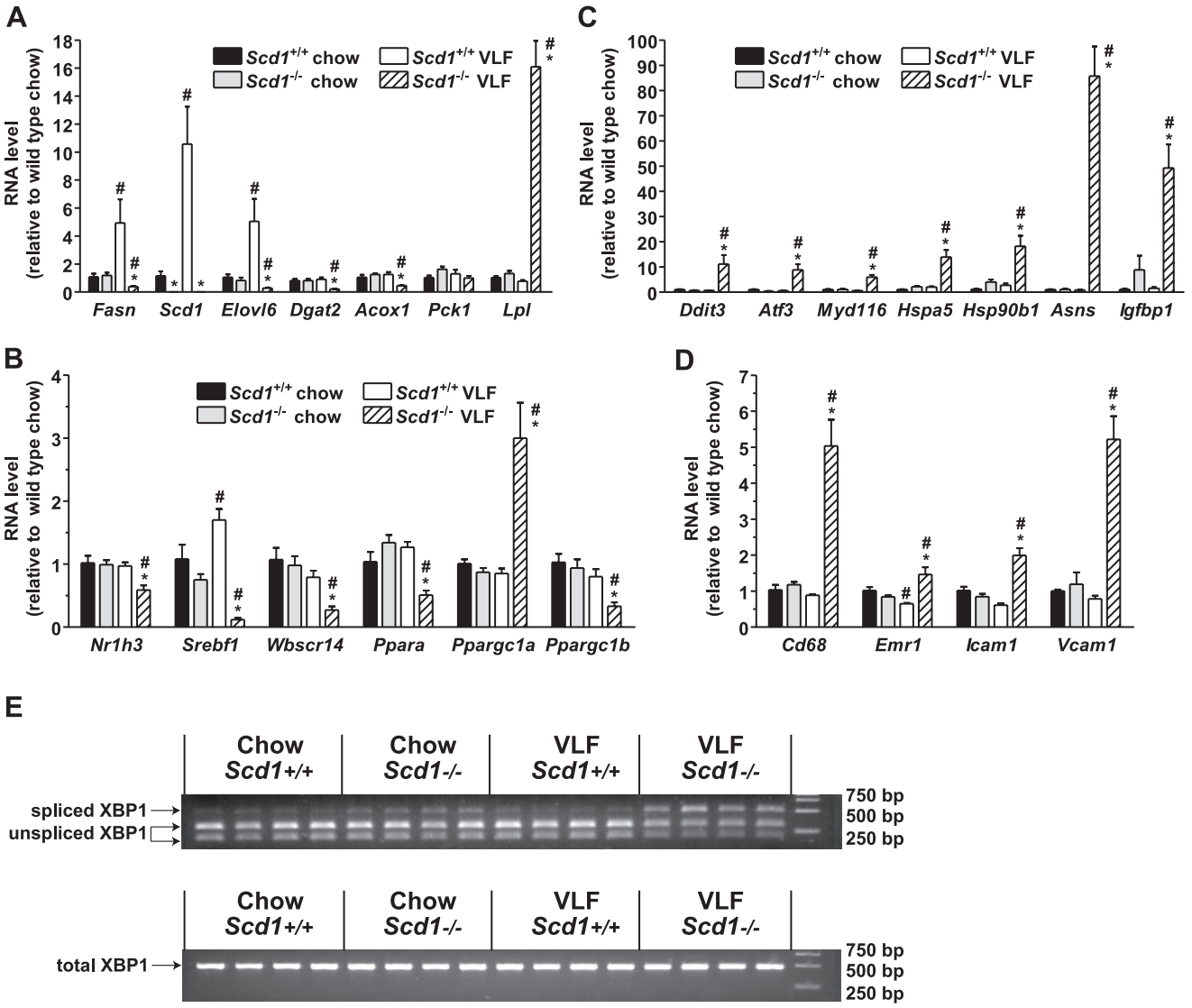

Fig. 3. Real-time PCR verification of select microarry targets and XBP1 splicing. Real-time quantitative PCR was performed on an ABI 7500 Fast instrument using gene-specific primers. Results are expressed as means ± SE for 5 mice per group. Data are presented relative to 185 ribosomal RNA in the same sample and categorized into metabolism (*A*), transcription (*B*), stress (*C*), and inflammation (*D*). *Genotype effect (within same diet); #diet effect (within same genotype). Data were analyzed by 2-way ANOVA with Bonferroni's postest and considered significant when $P < 0.05$. Primer sequences may be found in Supplementary Table S1. *E*: enhanced splicing of XBP1 mRNA in VLF *Scd1*$^{-/-}$ mice. XBP1 was amplified by PCR, digested with *Pst*1, and analyzed on a 2% agarose gel as described in METHODS *Pst*1 selectively cuts unspliced XBP1 into two fragments (*bottom* 2 bands), while spliced XBP1 lacks the restriction site and remains intact (*top* band). Each lane represents a single animal. Total XBP1 prior to *Pst1* digestion is shown as a loading control.

ER stress in tumor cells, but not normal fibroblasts, establishing a link between fatty acid synthesis and ER function (42). Furthermore, a recent study by Chakravarthy et al. (12) found that mice harboring a liver-specific deletion of FAS and fed a fat-free diet also had altered expression of genes involved in fatty acid oxidation, ketogenesis, and lipid transport. Since SCD1 is downstream of FAS, the effects of FAS inhibition may in part occur via reduced flux through SCD1. Additionally, exposure of liver cells to saturated, but not unsaturated, fatty acids has been shown to promote ER stress (73), and ER stress during hepatic steatosis is exacerbated by dietary changes that increase the hepatic content of saturated fatty acids (71). The mechanistic link between altered fatty acid composition and ER stress is currently not known but may be due to a disturbed physical state of cellular membranes. Altered fatty acid composition may alter the function and/or localization of membrane transport proteins. For example, the sarcoplasmic-ER calcium ATPase-2b, which requires conformational freedom to function properly, may be inhibited due to altered ER lipid composition resulting in loss of calcium from the ER (41). This could impair the function of certain calcium-dependent protein folding chaperones, such as BiP and calnexin, resulting in ER stress (43, 57, 68). It is also possible that the unsaturated fatty acid depletion causes ER stress by promoting cellular oxidative stress similar to the cholestatic symptoms observed in drug toxicity and ischemia (23, 64, 65). Alternatively, a primary defect in energy metabolism due to mitochondrial dysfunction or another mechanism may cause energy depletion and trigger an ER stress response (36).

The ER has a variety of mechanisms for sensing different forms of cellular stress. One branch, termed the integrated

stress response, involves translational repression via eIF2α phosphorylation by the eIF2α kinases PERK, GCN2, PKR, and HRI, which are activated by ER stress, amino acid deprivation, double-stranded viral RNA, and heme deficiency, respectively (64). In addition, the integrated stress response allows for selective translation of the mRNA encoding the transcription factor ATF4. The unfolded protein response in part acts through PERK and the integrated stress response but also promotes the posttranslational activation of ATF6 and IRE1, which mediate the two other branches of the cell stress response (36). We observed increased IRE1-dependent splicing of XBP1 mRNA in VLF *Scd1*$^{-/-}$ mice, indicating activation of the unfolded protein response. It is plausible that induction of the unfolded protein response, also evidenced by increased expression of *Hspa5* (BiP/GRP78), is responsible for the entire spectrum of ER stress-related gene expression changes (36). Interestingly, hepatic expression of the stress-induced transcription factor ATF3, which is induced by a variety of insults, has been shown to result in several symptoms of liver dysfunction, including hypoglycemia and increased serum levels of bilirubin, bile acids, and liver transaminases (3, 4). Thus, it is possible that the unsaturated fat deficiency is acting partly through an ATF3-dependent stress response pathway to cause the metabolic dysfunction in the VLF *Scd1*$^{-/-}$ mice.

Inflammation and dysregulation of nuclear hormone receptor expression. Unabated hepatic ER stress may lead to stimulation of inflammatory response pathways via activation of the inflammatory kinases c-Jun NH_2-terminal kinase and inhibitor of nuclear factor-κB kinase (31, 58, 76). This is of particular importance, since the acute inflammatory response has been shown to cause decreased expression of several nuclear hormone receptors and elicit major effects on lipid and lipoprotein metabolism (39, 40). This connection suggests that the decreased expression of nuclear hormone receptors and changes in mRNA levels of their target genes in the VLF *Scd1*$^{-/-}$ mice may be mediated via an inflammatory response acting through or independent of an intracellular ER stress signal. Future investigations are required to differentiate the upstream metabolic changes that cause the cellular stress response from those that are a downstream result of cellular stress and inflammation. Furthermore, changes in fatty acid composition resulting from the unsaturated fat deficiency in VLF *Scd1*$^{-/-}$ mice likely affect organelles other than the ER and various organs other than the liver. The unsaturated fat restriction from the 10-day VLF feeding may stimulate a systemic procatabolic inflammatory response to promote adipose lipolysis and muscle catabolism. This response occurs only in *Scd1*$^{-/-}$ mice, suggesting that de novo MUFA synthesis provides the metabolic flexibility to promote MUFA synthesis in times of dietary insufficiency.

In summary, our gene expression analysis of VLF *Scd1*$^{-/-}$ mice strongly suggests a novel link between unsaturated fatty acid insufficiency and cellular stress and inflammation pathways. These gene expression changes were dependent upon this diet-genotype interaction and did not occur in chow-fed *Scd1*$^{-/-}$ mice or in *Scd1*$^{+/+}$ mice fed the VLF diet. This illustrates that SCD1 resides at a critical junction in energy metabolism that allows not only for increased fatty acid biosynthesis in times of nutrient excess but also maintains cellular MUFA balance when deprived from the diet. Although the etiology of the MUFA deficiency phenotypes remains to be established, the overall pathology in this model has potential implications for future disease treatment interventions that target fatty acid biosynthesis.

ACKNOWLEDGMENTS

We thank the staff at the University of Wisconsin-Madison animal care facility, Kathryn L. Schueler for the maintenance of our mouse colony, and Dr. Annette Gendron-Fitzpatrick for liver histology. We thank Drs. Feroz Papa and Heather Harding for advice on the XBP1 splicing assay and eIF2α immunoblotting. We are also grateful to Drs. Albert Groen and Folkert Kuipers for careful reading of this manuscript and helpful discussions.

GRANTS

This work was supported by National Institutes of Health Grants HL-56593, DK-58037, DK-066369, and GM-076274.

REFERENCES

1. **Adrain AL, Ramberan H, Weaver GJ.** Evaluation of common liver problems. *J Am Podiatr Med Assoc* 94: 149–156, 2004.
2. **Al Sarraj J, Vinson C, Thiel G.** Regulation of asparagine synthetase gene transcription by the basic region leucine zipper transcription factors ATF5 and CHOP. *Biol Chem* 386: 873–879, 2005.
3. **Allen-Jennings AE, Hartman MG, Kociba GJ, Hai T.** The roles of ATF3 in glucose homeostasis. A transgenic mouse model with liver dysfunction and defects in endocrine pancreas. *J Biol Chem* 276: 29507–29514, 2001.
4. **Allen-Jennings AE, Hartman MG, Kociba GJ, Hai T.** The roles of ATF3 in liver dysfunction and the regulation of phosphoenolpyruvate carboxykinase gene expression. *J Biol Chem* 277: 20020–20025, 2002.
5. **Applied Biosystems.** *User Bulletin No. 2 Rev. B*. Forester City, CA: Applied Biosystems, 2001.
6. **Bavner A, Johansson L, Toresson G, Gustafsson JA, Treuter E.** A transcriptional inhibitor targeted by the atypical orphan nuclear receptor SHP. *EMBO Rep* 3: 478–484, 2002.
7. **Bernuau D, Moreau A, Tournier I, Legres L, Feldmann G.** Activation of nuclear protooncogenes and alpha-fetoprotein gene in rat liver during the acute inflammatory reaction. *Liver* 13: 102–109, 1993.
8. **Bligh EG, Dyer WJ.** A rapid method of total lipid extraction and purification. *Can J Biochem Physiol* 37: 911–917, 1959.
9. **Bruford EA, Lush MJ, Wright MW, Sneddon TP, Povey S, Birney E.** The HGNC Database in 2008: a resource for the human genome. *Nucleic Acids Res* 36: D445–D448, 2008.
10. **Busch AK, Gurisik E, Cordery DV, Sudlow M, Denyer GS, Laybutt DR, Hughes WE, Biden TJ.** Increased fatty acid desaturation and enhanced expression of stearoyl coenzyme A desaturase protects pancreatic beta-cells from lipoapoptosis. *Diabetes* 54: 2917–2924, 2005.
11. **Campbell KM, Sabla GE, Bezerra JA.** Transcriptional reprogramming in murine liver defines the physiologic consequences of biliary obstruction. *J Hepatol* 40: 14–23, 2004.
12. **Chakravarthy MV, Pan Z, Zhu Y, Tordjman K, Schneider JG, Coleman T, Turk J, Semenkovich CF.** "New" hepatic fat activates PPARalpha to maintain glucose, lipid, and cholesterol homeostasis. *Cell Metab* 1: 309–322, 2005.
13. **Cheng J, Sun S, Tracy A, Hubbell E, Morris J, Valmeekam V, Kimbrough A, Cline MS, Liu G, Shigeta R, Kulp D, Siani-Rose MA.** NetAffx Gene Ontology Mining Tool: a visual approach for microarray data analysis. *Bioinformatics* 20: 1462–1463, 2004.
14. **Corbacho AM, Valacchi G, Kubala L, Olano-Martin E, Schock BC, Kenny TP, Cross CE.** Tissue-specific gene expression of prolactin receptor in the acute-phase response induced by lipopolysaccharides. *Am J Physiol Endocrinol Metab* 287: E750–E757, 2004.
15. **Davis RA, Miyake JH, Hui TY, Spann NJ.** Regulation of cholesterol-7alpha-hydroxylase: BAREly missing a SHP. *J Lipid Res* 43: 533–543, 2002.
16. **Dobrzyn A, Dobrzyn P, Miyazaki M, Sampath H, Chu K, Ntambi JM.** Stearoyl-CoA desaturase 1 deficiency increases CTP:choline cytidylyltransferase translocation into the membrane and enhances phosphatidylcholine synthesis in liver. *J Biol Chem* 280: 23356–23362, 2005.
17. **Fernandez J, Lopez AB, Wang C, Mishra R, Zhou L, Yaman I, Snider MD, Hatzoglou M.** Transcriptional control of the arginine/lysine transporter, cat-1, by physiological stress. *J Biol Chem* 278: 50000–50009, 2003.

18. **Fickert P, Trauner M, Fuchsbichler A, Stumptner C, Zatloukal K, Denk H.** Cytokeratins as targets for bile acid-induced toxicity. *Am J Pathol* 160: 491–499, 2002.
19. **Finck BN, Kelly DP.** PGC-1 coactivators: inducible regulators of energy metabolism in health and disease. *J Clin Invest* 116: 615–622, 2006.
20. **Flowers JB, Rabaglia ME, Schueler KL, Flowers MT, Lan H, Keller MP, Ntambi JM, Attie AD.** Loss of stearoyl-CoA desaturase-1 improves insulin sensitivity in lean mice but worsens diabetes in leptin-deficient obese mice. *Diabetes* 56: 1228–1239, 2007.
21. **Flowers MT, Groen AK, Oler AT, Keller MP, Choi Y, Schueler KL, Richards OC, Lan H, Miyazaki M, Kuipers F, Kendziorski CM, Ntambi JM, Attie AD.** Cholestasis and hypercholesterolemia in SCD1-deficient mice fed a low-fat, high-carbohydrate diet. *J Lipid Res* 47: 2668–2680, 2006.
22. **Gachon F, Olela FF, Schaad O, Descombes P, Schibler U.** The circadian PAR-domain basic leucine zipper transcription factors DBP, TEF, and HLF modulate basal and inducible xenobiotic detoxification. *Cell Metab* 4: 25–36, 2006.
23. **Geier A, Wagner M, Dietrich CG, Trauner M.** Principles of hepatic organic anion transporter regulation during cholestasis, inflammation and liver regeneration. *Biochim Biophys Acta* 1773: 283–308, 2007.
24. **Gentleman RC, Carey VJ, Bates DM, Bolstad B, Dettling M, Dudoit S, Ellis B, Gautier L, Ge Y, Gentry J, Hornik K, Hothorn T, Huber W, Iacus S, Irizarry R, Leisch F, Li C, Maechler M, Rossini AJ, Sawitzki G, Smith C, Smyth G, Tierney L, Yang JY, Zhang J.** Bioconductor: open software development for computational biology and bioinformatics. *Genome Biol* 5: R80, 2004.
25. **Glibetic MD, Baumann H.** Influence of chronic inflammation on the level of mRNA for acute-phase reactants in the mouse liver. *J Immunol* 137: 1616–1622, 1986.
26. **Gray S, Wang B, Orihuela Y, Hong EG, Fisch S, Haldar S, Cline GW, Kim JK, Peroni OD, Kahn BB, Jain MK.** Regulation of gluconeogenesis by Kruppel-like factor 15. *Cell Metab* 5: 305–312, 2007.
27. **Harding HP, Novoa I, Zhang Y, Zeng H, Wek R, Schapira M, Ron D.** Regulated translation initiation controls stress-induced gene expression in mammalian cells. *Mol Cell* 6: 1099–1108, 2000.
28. **Harding HP, Zhang Y, Zeng H, Novoa I, Lu PD, Calfon M, Sadri N, Yun C, Popko B, Paules R, Stojdl DF, Bell JC, Hettmann T, Leiden JM, Ron D.** An integrated stress response regulates amino acid metabolism and resistance to oxidative stress. *Mol Cell* 11: 619–633, 2003.
29. **Haze K, Yoshida H, Yanagi H, Yura T, Mori K.** Mammalian transcription factor ATF6 is synthesized as a transmembrane protein and activated by proteolysis in response to endoplasmic reticulum stress. *Mol Biol Cell* 10: 3787–3799, 1999.
30. **Held MA, Cosme-Blanco W, Difedele LM, Bonkowski EL, Menon RK, Denson LA.** Alterations in growth hormone receptor abundance regulate growth hormone signaling in murine obstructive cholestasis. *Am J Physiol Gastrointest Liver Physiol* 288: G986–G993, 2005.
31. **Hotamisligil GS.** Inflammation and metabolic disorders. *Nature* 444: 860–867, 2006.
32. **Huang L, Mivechi NF, Moskophidis D.** Insights into regulation and function of the major stress-induced hsp70 molecular chaperone in vivo: analysis of mice with targeted gene disruption of the hsp70.1 or hsp703 *gene. Mol Cell Biol* 21: 8575–8591, 2001.
33. **Irizarry RA, Hobbs B, Collin F, Beazer-Barclay YD, Antonellis KJ, Scherf U, Speed TP.** Exploration, normalization, and summaries of high density oligonucleotide array probe level data. *Biostatistics* 4: 249–264, 2003.
34. **Jiang HY, Wek SA, McGrath BC, Lu D, Hai T, Harding HP, Wang X, Ron D, Cavener DR, Wek RC.** Activating transcription factor 3 is integral to the eukaryotic initiation factor 2 kinase stress response. *Mol Cell Biol* 24: 1365–1377, 2004.
35. **Jousse C, Deval C, Maurin AC, Parry L, Cherasse Y, Chaveroux C, Lefloch R, Lenormand P, Bruhat A, Fafournoux P.** TRB3 inhibits the transcriptional activation of stress-regulated genes by a negative feedback on the ATF4 pathway. *J Biol Chem* 282: 15851–15861, 2007.
36. **Kaufman RJ.** Orchestrating the unfolded protein response in health and disease. *J Clin Invest* 110: 1389–1398, 2002.
37. **Kendziorski CM, Newton MA, Lan H, Gould MN.** On parametric empirical Bayes methods for comparing multiple groups using replicated gene expression profiles. *Stat Med* 22: 3899–3914, 2003.
38. **Keum YS, Han YH, Liew C, Kim JH, Xu C, Yuan X, Shakarjian MP, Chong S, Kong AN.** Induction of heme oxygenase-1 (HO-1) and NAD[P]H: quinone oxidoreductase 1 (NQO1) by a phenolic antioxidant, butylated hydroxyanisole (BHA) and its metabolite, tert-butylhydroquinone (tBHQ) in primary-cultured human and rat hepatocytes. *Pharm Res* 23: 2586–2594, 2006.
39. **Khovidhunkit W, Kim MS, Memon RA, Shigenaga JK, Moser AH, Feingold KR, Grunfeld C.** Effects of infection and inflammation on lipid and lipoprotein metabolism: mechanisms and consequences to the host. *J Lipid Res* 45: 1169–1196, 2004.
40. **Kim MS, Sweeney TR, Shigenaga JK, Chui LG, Moser A, Grunfeld C, Feingold KR.** Tumor necrosis factor and interleukin 1 decrease RXRalpha, PPARalpha, PPARgamma, LXRalpha, and the coactivators SRC-1, PGC-1alpha, and PGC-1beta in liver cells. *Metabolism* 56: 267–279, 2007.
41. **Li Y, Ge M, Ciani L, Kuriakose G, Westover EJ, Dura M, Covey DF, Freed JH, Maxfield FR, Lytton J, Tabas I.** Enrichment of endoplasmic reticulum with cholesterol inhibits sarcoplasmic-endoplasmic reticulum calcium ATPase-2b activity in parallel with increased order of membrane lipids: implications for depletion of endoplasmic reticulum calcium stores and apoptosis in cholesterol-loaded macrophages. *J Biol Chem* 279: 37030–37039, 2004.
42. **Little JL, Wheeler FB, Fels DR, Koumenis C, Kridel SJ.** Inhibition of fatty acid synthase induces endoplasmic reticulum stress in tumor cells. *Cancer Res* 67: 1262–1269, 2007.
43. **Lodish HF, Kong N, Wikstrom L.** Calcium is required for folding of newly made subunits of the asialoglycoprotein receptor within the endoplasmic reticulum. *J Biol Chem* 267: 12753–12760, 1992.
44. **Marchand A, Tomkiewicz C, Magne L, Barouki R, Garlatti M.** Endoplasmic reticulum stress induction of insulin-like growth factor-binding protein-1 involves ATF4. *J Biol Chem* 281: 19124–19133, 2006.
45. **Merkel M, Weinstock PH, Chajek-Shaul T, Radner H, Yin B, Breslow JL, Goldberg IJ.** Lipoprotein lipase expression exclusively in liver. A mouse model for metabolism in the neonatal period and during cachexia. *J Clin Invest* 102: 893–901, 1998.
46. **Miyazaki M, Dobrzyn A, Man WC, Chu K, Sampath H, Kim HJ, Ntambi JM.** Stearoyl-CoA desaturase 1 gene expression is necessary for fructose-mediated induction of lipogenic gene expression by sterol regulatory element-binding protein-1c-dependent and -independent mechanisms. *J Biol Chem* 279: 25164–25171, 2004.
47. **Miyazaki M, Flowers MT, Sampath H, Chu K, Otzelberger C, Liu X, Ntambi JM.** Hepatic stearoyl-CoA desaturase-1 deficiency protects mice from carbohydrate-induced adiposity and hepatic steatosis. *Cell Metab* 6: 484–496, 2007.
48. **Miyazaki M, Kim YC, Ntambi JM.** A lipogenic diet in mice with a disruption of the stearoyl-CoA desaturase 1 gene reveals a stringent requirement of endogenous monounsaturated fatty acids for triglyceride synthesis. *J Lipid Res* 42: 1018–1024, 2001.
49. **Newton MA, Kendziorski CM, Richmond CS, Blattner FR, Tsui KW.** On differential variability of expression ratios: improving statistical inference about gene expression changes from microarray data. *J Comput Biol* 8: 37–52, 2001.
50. **Newton MA, Noueiry A, Sarkar D, Ahlquist P.** Detecting differential gene expression with a semiparametric hierarchical mixture method. *Biostatistics* 5: 155–176, 2004.
51. **Nishinaka T, Yabe-Nishimura C.** Transcription factor Nrf2 regulates promoter activity of mouse aldose reductase (AKR1B3) gene. *J Pharm Sci* 97: 43–51, 2005.
52. **Novoa I, Zhang Y, Zeng H, Jungreis R, Harding HP, Ron D.** Stress-induced gene expression requires programmed recovery from translational repression. *EMBO J* 22: 1180–1187, 2003.
53. **Ntambi JM, Miyazaki M.** Recent insights into stearoyl-CoA desaturase-1. *Curr Opin Lipidol* 14: 255–261, 2003.
54. **Ntambi JM, Miyazaki M, Stoehr JP, Lan H, Kendziorski CM, Yandell BS, Song Y, Cohen P, Friedman JM, Attie AD.** Loss of stearoyl-CoA desaturase-1 function protects mice against adiposity. *Proc Natl Acad Sci USA* 99: 11482–11486, 2002.
55. **Ohoka N, Yoshii S, Hattori T, Onozaki K, Hayashi H.** TRB3, a novel ER stress-inducible gene, is induced via ATF4-CHOP pathway and is involved in cell death. *EMBO J* 24: 1243–1255, 2005.
56. **Opherk C, Tronche F, Kellendonk C, Kohlmuller D, Schulze A, Schmid W, Schutz G.** Inactivation of the glucocorticoid receptor in hepatocytes leads to fasting hypoglycemia and ameliorates hyperglycemia in streptozotocin-induced diabetes mellitus. *Mol Endocrinol* 18: 1346–1353, 2004.
57. **Ou WJ, Bergeron JJ, Li Y, Kang CY, Thomas DY.** Conformational changes induced in the endoplasmic reticulum luminal domain of calnexin by Mg-ATP and Ca^{2+}. *J Biol Chem* 270: 18051–18059, 1995.

58. **Ozcan U, Cao Q, Yilmaz E, Lee AH, Iwakoshi NN, Ozdelen E, Tuncman G, Gorgun C, Glimcher LH, Hotamisligil GS.** Endoplasmic reticulum stress links obesity, insulin action, and type 2 diabetes. *Science* 306: 457–461, 2004.
59. **Parker MG, Christian M, White R.** The nuclear receptor co-repressor RIP140 controls the expression of metabolic gene networks. *Biochem Soc Trans* 34: 1103–1106, 2006.
60. **Pei L, Waki H, Vaitheesvaran B, Wilpitz DC, Kurland IJ, Tontonoz P.** NR4A orphan nuclear receptors are transcriptional regulators of hepatic glucose metabolism. *Nat Med* 12: 1048–1055, 2006.
61. **Pinnamaneni SK, Southgate RJ, Febbraio MA, Watt MJ.** Stearoyl CoA desaturase 1 is elevated in obesity but protects against fatty acid-induced skeletal muscle insulin resistance in vitro. *Diabetologia* 49: 3027–3037, 2006.
62. **R Development Core Team.** *R*: A language and environment for statistical computing. http://www.r-project.org. Vienna, Austria: R Foundation for Statistical Computing, 2005.
63. **Rhee J, Inoue Y, Yoon JC, Puigserver P, Fan M, Gonzalez FJ, Spiegelman BM.** Regulation of hepatic fasting response by PPARgamma coactivator-1alpha (PGC-1): requirement for hepatocyte nuclear factor 4alpha in gluconeogenesis. *Proc Natl Acad Sci USA* 100: 4012–4017, 2003.
64. **Ron D.** Translational control in the endoplasmic reticulum stress response. *J Clin Invest* 110: 1383–1388, 2002.
65. **Sekine S, Ito K, Horie T.** Oxidative stress and Mrp2 internalization. *Free Radic Biol Med* 40: 2166–2174, 2006.
66. **Smyth GK.** Linear models and empirical bayes methods for assessing differential expression in microarray experiments. *Stat Appl Genet Mol Biol* 3: 2004.
67. **Sugden MC, Holness MJ.** Mechanisms underlying regulation of the expression and activities of the mammalian pyruvate dehydrogenase kinases. *Arch Physiol Biochem* 112: 139–149, 2006.
68. **Suzuki CK, Bonifacino JS, Lin AY, Davis MM, Klausner RD.** Regulating the retention of T-cell receptor alpha chain variants within the endoplasmic reticulum: Ca^{2+}-dependent association with BiP. *J Cell Biol* 114: 189–205, 1991.
69. **Tal M, Schneider DL, Thorens B, Lodish HF.** Restricted expression of the erythroid/brain glucose transporter isoform to perivenous hepatocytes in rats. Modulation by glucose. *J Clin Invest* 86: 986–992, 1990.
70. **Wan YJ, An D, Cai Y, Repa JJ, Hung-Po Chen T, Flores M, Postic C, Magnuson MA, Chen J, Chien KR, French S, Mangelsdorf DJ, Sucov HM**. Hepatocyte-specific mutation establishes retinoid X receptor alpha as a heterodimeric integrator of multiple physiological processes in the liver. *Mol Cell Biol* 20: 4436–4444, 2000.
71. **Wang D, Wei Y, Pagliassotti MJ.** Saturated fatty acids promote endoplasmic reticulum stress and liver injury in rats with hepatic steatosis. *Endocrinology* 147: 943–951, 2006.
72. **Wang Y, Lam KS, Kraegen EW, Sweeney G, Zhang J, Tso AW, Chow WS, Wat NM, Xu JY, Hoo RL, Xu A.** Lipocalin-2 is an inflammatory marker closely associated with obesity, insulin resistance, and hyperglycemia in humans. *Clin Chem* 53: 34–41, 2007.
73. **Wei Y, Wang D, Topczewski F, Pagliassotti MJ.** Saturated fatty acids induce endoplasmic reticulum stress and apoptosis independently of ceramide in liver cells. *Am J Physiol Endocrinol Metab* 291: E275–E281, 2006.
74. **Yang J, Croniger CM, Lekstrom-Himes J, Zhang P, Fenyus M, Tenen DG, Darlington GJ, Hanson RW.** Metabolic response of mice to a postnatal ablation of CCAAT/enhancer-binding protein alpha. *J Biol Chem* 280: 38689–38699, 2005.
75. **Yu J, Koenig RJ.** Induction of type 1 iodothyronine deiodinase to prevent the nonthyroidal illness syndrome in mice. *Endocrinology* 147: 3580–3585, 2006.
76. **Zhang K, Shen X, Wu J, Sakaki K, Saunders T, Rutkowski DT, Back SH, Kaufman RJ.** Endoplasmic reticulum stress activates cleavage of CREBH to induce a systemic inflammatory response. *Cell* 124: 587–599, 2006.